



## EFFECT OF FIBER ORIENTATION ON THE ROOT STRESSES OF THE GEAR TOOTH

Assist. Prof. Mohammad Q. Abdullah  
Mechanical Engineering  
University of Baghdad

Issam Shamouael  
Mechanical Engineering  
University of Baghdad

### ABSTRACT

The effect of fiber orientation angle of composite materials on the gear tooth root stresses is analytically investigated in order to select the required orientation of the fibers inside the gear tooth, which leads to improve the gear tooth strength. The effect of geometrical parameters (loaded or unloaded pressure angles, number of teeth, radius of fillet and profile correction) and type of fibers (glass, graphite and boron) are also studied. A stress analysis using the finite element method is performed for reinforced gear subject to bending loads. The results indicate that there is an effect of the fiber orientation on the root stresses of the gear tooth, and also, there is a direct proportionality between the improving of the gear strength with geometrical parameters.

### الخلاصة

في هذا البحث تم دراسة تأثير توجه الألياف للمواد المركبة على اجهادات الجذر لأسنان التروس لغرض اختيار الزاوية المطلوبة للألياف داخل أسنان التروس والتي تؤدي إلى تحسين مقاومة الأسنان للأحمال. وتم أيضاً دراسة تأثير الأبعاد الهندسية التصميمية Geometrical Parameters (زاوية الضغط المحملة والغير محملة ، عدد أسنان الترس ، نصف قطر المتكأ الزاوي ومعامل التصحيح) وكذلك تأثير نوع الألياف المستخدمة (زجاج ، جرافيت ، بورون). وقد تم إجراء التحليل العددي باستخدام طريقة العناصر المحددة للحصول على توزيع الاجهادات داخل أسنان التروس. وقد اتضح من النتائج المستحصلة بان اتجاه الألياف يؤثر على اجهادات الجذر لاسنان التروس، وكذلك اتضح من النتائج بأن هناك علاقة مباشرة بين اجهادات الجذر مع الأبعاد الهندسية التصميمية.

### KEY WORDS

Gear, finite element, composite materials, fiber reinforcement

### INTRODUCTION

One of the primary causes of gear tooth failures is the presence of large tensile stresses in the root fillets of loaded gear teeth. These stresses tend to reduce overall gear life and can result in catastrophic tooth failure under peak loading conditions. Therefore, many methods are investigated to improve the strength of gear teeth, one of these methods is to reinforce the gear teeth with fibers as shown in Fig. (1).

Many attempts have been made by earlier investigations to relate tensile fillet stresses observed in statically loaded gear teeth to the geometric appearance of the tooth.

[Wilfred Lewis, 1892] applied elementary beam theory to symmetrical tooth profiles by inscribing a parabola to represent a beam of uniform strength. As a result of the uniform strength assumption the Lewis formula was unable to deal effectively with abrupt changes in tooth section that occur in the tooth fillet region. Furthermore, for teeth with high-pressure angles a radial component of load exists that tends to modify the stress produced by the applied bending moment.

[Merritt, 1952] added a term to the Lewis formula that accounted for the radial component of load, which was assumed to act along the vertical centerline of the symmetric tooth. At this point neither the Lewis nor the Merritt formulas was able to take into account abrupt changes in tooth section and neither was applicable to teeth with unbalanced pressure angle.

[Dolan and Broghamer, 1942] studied the subject in depth and introduced a combined stress correction and stress concentration factor to be used in conjunction with the Lewis stress formula. This factor related the increase in observed fillet stress over the nominal bending stress to load height, fillet radius and pressure angle.

[Satoshi oda, 1986] investigated the tooth deflection and bending stresses at root fillet due to concentrated load on a gear tooth of long tooth with various pressure angles using the finite difference method (FDM).

[Mohammad Q. Abdullah, 1994] studied the analysis of gear tooth stresses using finite element technique. Result indicate that the unsymmetrical gear tooth with loaded side pressure angle  $14.5^\circ$  and unloaded side pressure angle  $20^\circ$  or  $25^\circ$  is better than the symmetrical tooth of standards pressure angles of  $14.5^\circ$  or  $20^\circ$  or  $25^\circ$  from the point of view of strength, dynamic loads and generated noise.

[Kozo Ikegami and Kenji Kikushima, 1986] studied the effects of material constitutions on the strength of fiber reinforced plastic gears. A method to reinforce gear teeth with glass or carbon roving cloths along the tooth profile is proposed to improve the bending strength. A stress analysis using the finite element method is performed for reinforced gears subjected to bending loads. Various fiber systems are considered and strengths are estimated. From these results, the strengthening effects are shown that fiber reinforcement is useful to improve the strength of plastic gears.

The main objective of this paper is to investigate the effect of fiber orientation angle of composite materials on the root stresses of the gear tooth. To achieve this work, the following steps will be followed:

- 1- Built up a finite element program for general orthotropic material to carryout the stress analysis for plane strain condition. The element used in the analysis is 8-node isoparametric element with 2-degrees of freedom at each node. MSC/NASTRAN package will be used to check the validity of the program.
- 2- The effect of pressure angle, number of teeth, fillet radius, positive profile correction, and the type of fiber were investigated under static loading.

### THEORITICAL ANALYSIS OF A LAMINA

For a lamina in the (1-2) plane as shown in Fig. (2), a plane strain state is defined by setting

$$\varepsilon_3 = 0, \quad \tau_{23} = 0, \quad \tau_{13} = 0 \quad \dots (1)$$

therefore, the strain stress relations for orthotropic material are [Robert M. Jones, 1975]:

$$\begin{Bmatrix} \varepsilon_1 \\ \varepsilon_2 \\ \gamma_{12} \end{Bmatrix} = \begin{bmatrix} S_{11} & S_{12} & 0 \\ S_{12} & S_{22} & 0 \\ 0 & 0 & S_{66} \end{bmatrix} \begin{Bmatrix} \sigma_1 \\ \sigma_2 \\ \tau_{12} \end{Bmatrix} \quad \dots (2)$$

For the case of transversely isotropic, the following material conditions can be employed (plane 2-3 is the plane of isotropy Fig. (2)):



$$E_3 = E_2, \quad \nu_{13} = \nu_{12}, \quad G_{13} = G_{12}, \quad \text{and} \quad G_{23} = \frac{E_2}{2(1 + \nu_{23})}$$

Therefore, the strain-stress constants ( $s_{ij}$ ) become:

$$\begin{aligned} S_{11} &= \frac{1}{E_1} (1 - \nu_{12}^2 \frac{E_2}{E_1}) \\ S_{12} &= -\frac{\nu_{12}}{E_1} (1 + \nu_{23}) = -\frac{\nu_{21}}{E_2} (1 + \nu_{23}) \\ S_{22} &= \frac{1}{E_2} (1 - \nu_{23}^2) \quad \dots (3) \\ S_{66} &= \frac{1}{G_{12}} \end{aligned}$$

The strain-stress relations in Eq. (2) can be inverted to obtain the stress-strain relations:

$$\begin{Bmatrix} \sigma_1 \\ \sigma_2 \\ \tau_{12} \end{Bmatrix} = \begin{bmatrix} Q_{11} & Q_{12} & 0 \\ Q_{12} & Q_{22} & 0 \\ 0 & 0 & Q_{66} \end{bmatrix} \begin{Bmatrix} \varepsilon_1 \\ \varepsilon_2 \\ \gamma_{12} \end{Bmatrix} \quad \dots (4)$$

where the  $Q_{ij}$ , the so-called reduced stiffnesses, are

$$\begin{aligned} Q_{11} &= \frac{E_1}{\Delta} (1 - \nu_{23}^2) \\ Q_{12} &= \frac{\nu_{12}}{\Delta} (1 + \nu_{23}) \\ Q_{22} &= \frac{1}{\Delta} (1 - \nu_{12}^2 \frac{E_2}{E_1}) \quad \dots (5) \\ Q_{66} &= G_{12} \end{aligned}$$

$$\text{where, } \Delta = \left( \frac{1}{E_2} - \frac{\nu_{12}^2}{E_1} \right) (1 - \nu_{23}^2) - \frac{\nu_{12}^2}{E_1} (1 + \nu_{23})^2$$

### STRESS-STRAIN RELATION FOR A LAMINA OF ARBITRARY ORIENTATION

In the previous section stresses and strains were defined in the principal material directions for an orthotropic material. However, the principal directions of orthotropy often do not coincide with coordinate directions that are geometrically nature to the solution of the problem, as shown in Fig. (3). Thus a relation is needed between the stresses and strains in the principal material directions and those in the body coordinates. Then, a method of transforming stress-strain relations from one coordinate system to another is also needed.

At this point, we recall from elementary mechanics of material the transformation equations for expressing stresses in a x-y coordinate system in terms of stresses in a 1-2 coordinate system [Robert M. Jones, 1975],

$$\begin{Bmatrix} \sigma_x \\ \sigma_y \\ \tau_{xy} \end{Bmatrix} = \begin{bmatrix} \cos^2 \theta & \sin^2 \theta & -2 \sin \theta \cos \theta \\ \sin^2 \theta & \cos^2 \theta & 2 \sin \theta \cos \theta \\ \sin \theta \cos \theta & -\sin \theta \cos \theta & \cos^2 \theta - \sin^2 \theta \end{bmatrix} \begin{Bmatrix} \sigma_1 \\ \sigma_2 \\ \tau_{12} \end{Bmatrix} \quad \dots (6)$$

where  $\theta$  is the angle from the x-axis to the 1-axis see **Fig. (3)**). Note especially that the transformation has nothing to do with the material properties but is merely a rotation of stresses. Similarly, the stress-strain relations in x-y coordinates are:

$$\begin{Bmatrix} \sigma_x \\ \sigma_y \\ \tau_{xy} \end{Bmatrix} = [\bar{Q}] \begin{Bmatrix} \epsilon_x \\ \epsilon_y \\ \gamma_{xy} \end{Bmatrix} = \begin{bmatrix} \bar{Q}_{11} & \bar{Q}_{12} & \bar{Q}_{16} \\ \bar{Q}_{12} & \bar{Q}_{22} & \bar{Q}_{26} \\ \bar{Q}_{16} & \bar{Q}_{26} & \bar{Q}_{66} \end{bmatrix} \begin{Bmatrix} \epsilon_x \\ \epsilon_y \\ \gamma_{xy} \end{Bmatrix} \quad \dots (7)$$

in which

$$\begin{aligned} \bar{Q}_{11} &= Q_{11} \cos^4 \theta + 2(Q_{12} + 2Q_{66}) \sin^2 \theta \cos^2 \theta + Q_{22} \sin^4 \theta \\ \bar{Q}_{12} &= (Q_{11} + Q_{22} - 4Q_{66}) \sin^2 \theta \cos^2 \theta + Q_{12} (\sin^4 \theta + \cos^4 \theta) \\ \bar{Q}_{22} &= Q_{11} \sin^4 \theta + 2(Q_{12} + 2Q_{66}) \sin^2 \theta \cos^2 \theta + Q_{22} \cos^4 \theta \\ \bar{Q}_{16} &= (Q_{11} - Q_{12} - 2Q_{66}) \sin \theta \cos^3 \theta + (Q_{12} - Q_{22} + 2Q_{66}) \sin^3 \theta \cos \theta \\ \bar{Q}_{26} &= (Q_{11} - Q_{12} - 2Q_{66}) \sin^3 \theta \cos \theta + (Q_{12} - Q_{22} + 2Q_{66}) \sin \theta \cos^3 \theta \\ \bar{Q}_{66} &= (Q_{11} + Q_{12} - 2Q_{66}) \sin^2 \theta \cos^2 \theta + Q_{66} (\sin^4 \theta + \cos^4 \theta) \end{aligned} \quad \dots (8)$$

where the bar over the  $\bar{Q}_{ij}$  matrix denotes that we are dealing with the transformed reduced stiffnesses instead of the reduced stiffnesses  $Q_{ij}$ . Note that the transformed reduced stiffness matrix  $\bar{Q}_{ij}$  has terms in all nine positions in contrast to the presence of zeros in the reduced stiffness matrix  $Q_{ij}$ .

### STRENGTH ANALYSIS FOR AN ORTHOTROPIC LAMINA

Most experimental determinations of the strength of a material are based on uniaxial stress state. However, the general practical problem involves a biaxial and a triaxial state of stress. Thus, a logical method of using uniaxial strength information in the analysis of multiaxial loading problems is required.

However, there are at least a hundred of failure criteria, which may be used to assess the composite ply strength under a multi-axial stress system. The best failure criteria are those, which correlate with experimental values, the most commonly used are:

- 1- Maximum stress theory.
- 2- Maximum strain theory.
- 3- Tsai-Hill theory.
- 4- Tsai-Wu tensor theory.





5- Hoffman theory.

In all theories, the material, although orthotropic, must be homogeneous. Thus, some of the microscopic failure mechanisms inherently cannot be accounted for. At the same time, the strength theories tend to be smoother than the actual behavior which often exhibits considerable data scatter due to testing technique, manufacturing nonuniformities, [Robert M. Jones, 1975].

However, our attention for the current work will be restricted to Hoffman theory because it is obviously of more general character than the other theories and also it takes into account the different of tension and compression failure strengths. The relation which describes this theory is as:

$$Failure\ Index = \left( \frac{\sigma_1}{X_t} - \frac{\sigma_1^2}{X_t X_c} + \frac{\sigma_1}{X_c} \right) + \left( \frac{\sigma_2}{Y_t} - \frac{\sigma_2^2}{Y_t Y_c} + \frac{\sigma_2}{Y_c} \right) + \frac{\tau_{12}^2}{S^2} + \frac{\sigma_1 \sigma_2}{X_t X_c} \quad \dots (9)$$

where:

$\sigma_1$  normal stress in 1-direction.

$\sigma_2$  transverse stress in 2-direction.

$\tau_{12}$  shear stress in (1-2) plane.

And also,

$X_t (X_c)$  axial or longitudinal tensile (compressive) strength in the 1-direction.

$Y_t (Y_c)$  transverse tensile (compressive) strength in the 2-direction.

$S$  shear strength in the (1-2) plane.

And from this relation, the failure occurs when:

$$Failure\ Index (F.I) \geq 1$$

### FORMULATION OF LOADING ANGLE “β”

The loading angle “β” of the normal applied force “F”, should be determined at the tip of the gear tooth for each pressure angle and number of teeth on the loaded side of the investigated tooth, because the horizontal and vertical force components, “F<sub>x</sub>” and “F<sub>y</sub>” of the normal applied force are required as an input data for the finite element program [Nema Khalifa AL-ID, 1987].

$$\beta = \cos^{-1} \left( \frac{R_p}{R_a} \cos \phi \right) - \frac{\pi}{2z} - (\tan \phi - \phi) + (\tan \theta' - \theta') \quad \dots (10)$$

where  $\phi$  represents the pressure angle for the loaded side of tooth.

### FINITE ELEMENT ANALYSIS

In the finite element method, the actual domain of the gear tooth represented as an assemblage of sub-divisions called “finite elements”. These elements are considered to be interconnected at specified joints, which are called “nodes” or “nodal points”. The nodes usually lie on the element boundaries where adjacent elements are considered to be connected. Since the actual variation of the field variable (such as displacement components) inside the domain is not known, it can be assumed that the variation of the field variable inside a finite element can be approximated by a simple function. These approximating functions (which are called interpolating models) are defined in terms of values of the field variables at the nodes. When field equations (such as equilibrium equations) for the whole gear tooth are written, the new unknowns will be the nodal values of the field variable. By solving the field equations, which are generally in the form of matrix equations, the nodal values of the field variable will be known. Once these are the approximating functions

define the field variable throughout the assemblage of elements. The first step in the finite element method is to divide the whole domain of the gear into sub-divisions or elements. Hence the gear tooth that is being analyzed has to be modeled with suitable finite elements. The number, type, size and arrangement of the elements have to be decided.

Gear tooth profile program (GTP) [Mohammad Q. Abdullah, 1994] has been used to generate symmetrical and unsymmetrical spur gear teeth for different pressure angle, different number of teeth, and with or without correction. Fig. (4) shows six samples of this program.

Gear auto mesh program (GAM) has been built up in order to generate nodes with known coordinates (x & y) and also to generate elements of 8-nodes inside the gear tooth domain. Fig. (5) present two samples of the studied cases, which are generated by using (GTP) and (GAM) programs.

The finite element mesh that have been used in this work contains 387 nodes, 108 elements each element has 8 node and each node has two degree of freedom (isoparametric element) as shown in Fig. (4). The boundary condition can be shown in Fig. (6) where all the nodes along the sides' (b) and (c) are fixed in x-direction but can be moved in y-direction, and all the nodes in side (a) are fixed in y-direction but can be moved in x-direction.

#### VALIDITY TEST OF FEM PROGRAM

Because there is no an exact solution (analytical solution) or experimental results to compare with FEM program's results. Therefore, the validity of the program will be achieved by comparing its results with the available results published in the literatures, i.e. [Kozo Ikegami and Kenji Kikushima, 1986].

The studied gear is a spur gear of module 5, pressure angle 20° with number of teeth 30. For the stress analysis, the finite element method is used assuming a plane strain condition. Fig. (7) shows a method of the studied gear. A concentrated normal load of 10 N/mm is applied at the top of the gear tooth. In Fig. (7), region (1) is a resin rich zone, regions (2) to (4) are the fiber cloth reinforced parts and region (5) is the chopped fiber reinforced part.

The stress distribution for a given applied load is calculated by using the material constants of the gear elements. The theory of failure which is used in this analysis is the maximum stress theory, i.e. ply failure will occur if any stress in the material axes directions exceeds the respective basic failure strength:

$$\frac{\sigma_1}{X} < 1 \quad , \quad \frac{\sigma_2}{Y} < 1 \quad \text{and} \quad \frac{\tau_{12}}{S} < 1$$

where: X, Y : axial and transverse strength in 1 and 2 direction respectively.

S : shear strength in the (1-2) plane.

The mesh model which is used in this case, consists of 864 isoparametric elements with two degree of freedom and 8-nodes.

Table (1) shows the comparison between [Kozo Ikegami and Kenji Kikushima, 1986] and FEM program's results, where for case (1) carbon fabric in the regions 2,3, and 4 and glass chop in the region 5, while for case (2) glass fabric in the regions 2,3, and 4 and glass chop in the region 5.

The comparison shows that there is good agreement between [Kozo Ikegami and Kenji Kikushima, 1986] and FEM program, therefore, the validity of the FEM program is satisfied.



Table (1) Validity Test for FEM Program.

		Max. ( $\sigma_1/X$ )	Max. ( $\sigma_2/Y$ )	Max. ( $\tau_{12}/S$ )
Case (1)	Ref. [5]	0.023	0.074	0.009
	FEM program	0.021049	0.066958	0.008381
	Percentage Error	8.48%	9.52%	6.88%
Case (2)	Ref. [5]	0.057	0.0275	0.0075
	FEM program	0.052159	0.024885	0.006982
	Percentage Error	8.49%	9.51%	6.91%

### STUDIED CASES

From the Fig. (8) many parameters affect the gear tooth shape like pressure angle ( $\phi$ ), number of teeth ( $Z$ ), radius of fillet ( $R$ ) and positive profile correction ( $x$ ). Therefore, to achieve the above objectives, the effects of fiber orientation with varying all of these parameters have been studied.

The studied cases can be summarized as follows:

- 1- Varying the pressure angles, the pressure angles are selected to be one of the following available standard values  $14.5^\circ$ ,  $20^\circ$  and  $25^\circ$ .

(a)

$$\phi_u = \phi_\ell = 14.5^\circ$$

$$\phi_u = \phi_\ell = 20^\circ$$

$$\phi_u = \phi_\ell = 25^\circ$$

(b)

$$\phi_u = 14.5^\circ - \phi_\ell = 14.5^\circ$$

$$\phi_u = 20^\circ - \phi_\ell = 14.5^\circ$$

$$\phi_u = 25^\circ - \phi_\ell = 14.5^\circ$$

(c)

$$\phi_u = 20^\circ - \phi_\ell = 20^\circ$$

$$\phi_u = 25^\circ - \phi_\ell = 20^\circ$$

- 2- Varying the number of teeth,  $Z=(14, 19, \text{ and } 24)$  tooth.

- 3- Varying the radius of fillet

$$r_f = 0.3 m_o, 0.4 m_o, 0.6 m_o$$

- 4- Effect of profile correction.

(a) for  $Z=14, \phi=14.5^\circ$

without correction  $x=0$

with correction  $x=0.56$

(b) for  $Z=14, \phi=20^\circ$

without correction  $x=0$

with correction  $x=0.18$

5- 5. Effect of various fibers reinforced gear tooth. Three types of fiber have been studied (Glass, Graphite, Boron) fiber.

The tooth geometry, material properties, loading conditions, boundary conditions and plane symmetry condition are as follows:

#### Geometry

Module,  $m_o = 10\text{mm}$

Tooth face width,  $b = 1\text{mm}$

Addendum height,  $h_a = m_o = 10\text{mm}$

Dedendum height,  $h_d = 1.25 m_o = 12.5\text{mm}$

#### Mechanical Properties of Materials

Table (2) gives the elastic moduli and strength of materials used in the unidirectional fiber reinforced gears.

#### Loading Condition

An external normal force "F" of 50 N per unit face width "b" is applied at the tooth tip with an angle " $\beta$ ". The value of the applied force is selected such that the values of failure index (F.I.) with the varying of fiber orientations will be clear at the tension and compression sides of gear tooth.

#### Boundary conditions

As stated before.

#### Plane symmetry condition

The gear tooth domain is considered as a plane strain problem.

### FINITE ELEMENT RESULTS

The basic aim of the FEM program is to obtain the stress distribution, the maximum failure index (using Hoffman Criteria) for each orientation of fiber inside the gear tooth domain which is considered as a plane strain problem, under the stated load and boundary conditions. The material of the gear tooth, which is considered as a reference case for the finite element results, is Glass/Epoxy.

A symmetrical gear tooth with  $\phi_l = \phi_u = 20^\circ$ ,  $Z = 19$  teeth,  $r_f = 0.3 m_o$  and  $x = 0$  of fiber glass type will be taken as a benchmark case for the validity tests for FEM program. In addition to the validity test which described before, the computational efficiency of the FEM program will be achieved again by comparing its result with MSC/NASTRAN package. **Table (3)** contains the maximum values of the failure index at ( $\theta = 120^\circ$  &  $75^\circ$ ) for tension and compression sides respectively of FEM program and MSC/NASTRAN package. **Fig. (9)** show the effect of fiber orientation on the failure index for FEM program and MSC/NASTRAN package for both tension and compression sides. **Fig. (10)** shows the effect of fiber orientation on the failure index (F.I.) for tension and compression sides. To show the effect of the pressure angle on the failure index in this work, three standard values ( $14.5^\circ$ ,  $20^\circ$  and  $25^\circ$ ) of pressure angle have been studied. **Fig. (11)** shows the effect of the symmetrical pressure angles on the failure index and also, **Fig. (12)** shows the effect of unsymmetrical pressure angles on the (F.I.), where the solid lines represent the tension side while the dotted lines represent the compression side.

The effects of number of teeth, radius of fillet, profile correction, and type of fiber reinforced material on the failure index are shown in **Figs. (13) to (15)**.



## DISCUSSION

From the percentage errors were computed between the present work and MSC/NASTRAN package, as shown in **Table (3)** and **Fig. (9)**. It's noted that the percentage error was small between the results, therefore, the validity of the FEM program was satisfied. From **Fig. (10)**, it could be recognized that the failure index has the smallest value when the fiber orientation lies between ( $110^\circ - 120^\circ$ ) at tension side and ( $60^\circ - 75^\circ$ ) at compression side, i.e. when the fiber is parallel to the tooth profile at the weakest section point. It is clear that the increase of the tooth strength i.e. decreasing the failure index at the root fillets are directly proportional with the increase of the following geometrical parameters:-

- 1- The loaded and /or unloaded sides pressure angles.
- 2- The number of teeth.
- 3- The fillet radius.
- 4- The profile correction.

Where the increase in the above parameters will lead to increase the critical cross-sectional area of the gear tooth, as shown in **Figs. (11) to (14)**.

From **Fig. (15)**, it is clear that the reinforcement of gear tooth with boron fiber will lead to decrease the failure index more than using graphite or glass fiber, but at  $\theta = 120^\circ$  at tension side and  $\theta = 60^\circ$  at compression side, the reinforcement with graphite fiber is better than the boron fiber.

## CONCLUSIONS

The main conclusions obtained from the present analysis can be summarized as follows: -

- 1- There is an effect of the fiber orientation on the root stresses (which represented by the failure index) of the gear tooth. Where the failure index has a minimum value when  $\theta = (105^\circ \text{ to } 120^\circ)$  at the tension side, and when  $\theta = (60^\circ \text{ to } 75^\circ)$  at the compression side.
- 2- There is a direct proportionality between the improving of the root stresses of the gear tooth with the geometrical parameters (loaded and unloaded pressure angles, number of teeth, radius of fillet and profile correction). Where the increase in these geometrical parameters leads to decrease the failure index.
- 3- There is an effect for the fiber type of the reinforced gear tooth on its root stresses. Where the reinforced gear tooth with boron fiber are better than glass or graphite fiber from the point of view of root stresses (failure index).

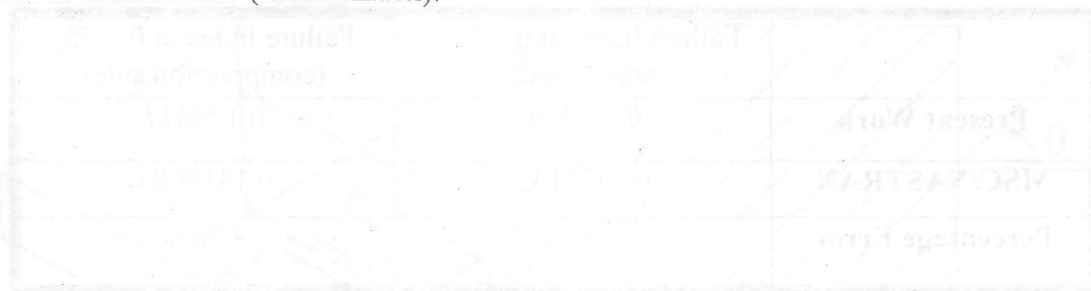


Table (2) Material Constants used in the Gear Analysis

Material Constants	Matrix	Glass/ Epoxy	Graphite/ Epoxy	Boron/ Epoxy
Young's modulus (Gpa)				
E1	3.38	53.77911	206.8427	206.8427
E2	3.38	17.92637	5.171068	20.68427
Shear modulus (Gpa)				
G12	1.225	8.963184	2.585534	6.894757
Poisson's ratio				
$\nu_{12}$	0.38	0.25	0.25	0.3
Tensile strength (Mpa)				
$X_t$	29	1034.214	1034.214	1378.951
$Y_t$	29	27.57903	41.36854	82.73709
Compressive strength (Mpa)				
$X_c$	158	1034.214	689.4757	2757.903
$Y_c$	158	137.8951	117.2109	275.7903
Shear Strength (Mpa)				
$S_{12}$	83	41.36854	68.94757	124.1056

Table (3) Verification Test for Static Case.

	Failure Index at $\theta = 120^\circ$ (tension side)	Failure Index at $\theta = 75^\circ$ (compression side)
<b>Present Work</b>	0.159828	0.125627
<b>MSC/NASTRAN</b>	0.1726142	0.1319083
<b>Percentage Error</b>	7.41%	4.76%

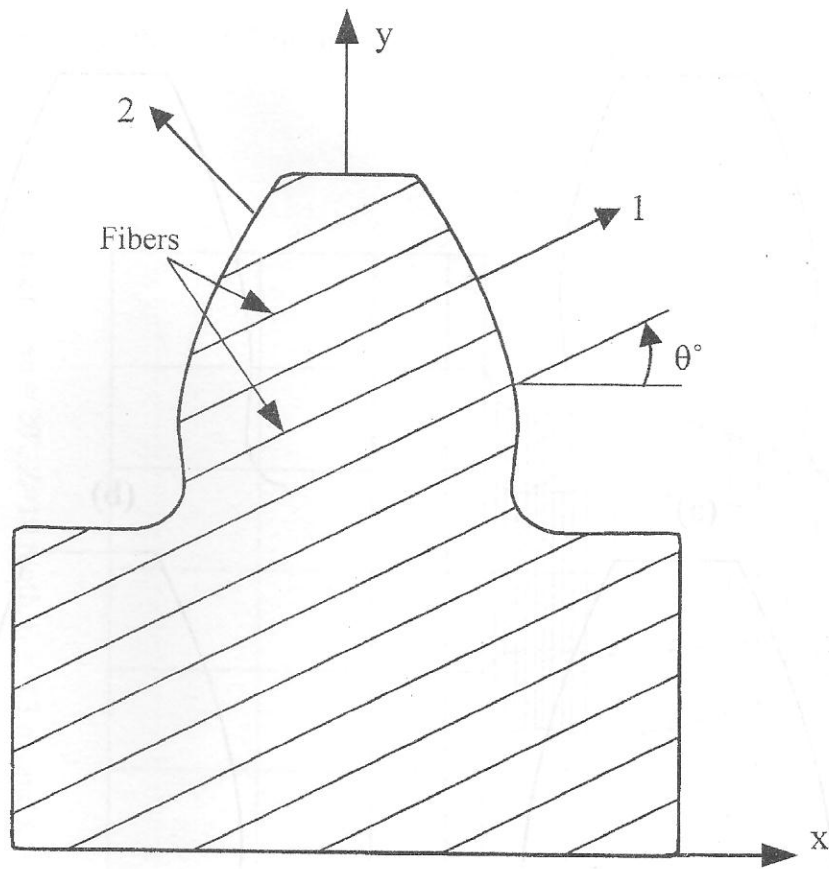


Fig. (1) Reinforcement of the Gear Tooth with Fibers.

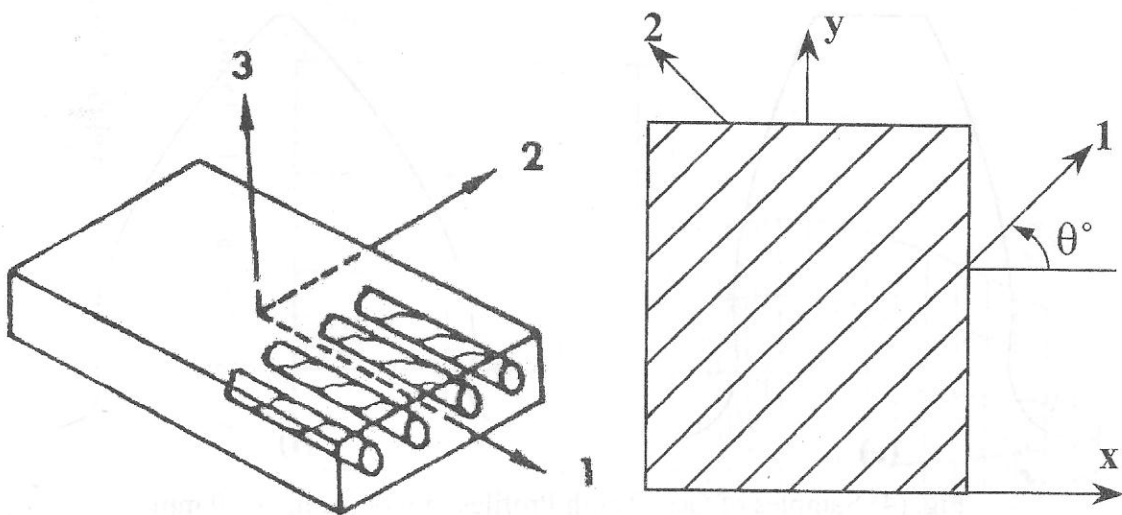


Fig. (2) Unidirectionally Reinforced lamina.

Fig. (3) Lamina of arbitrary orientation of Principal material directions.

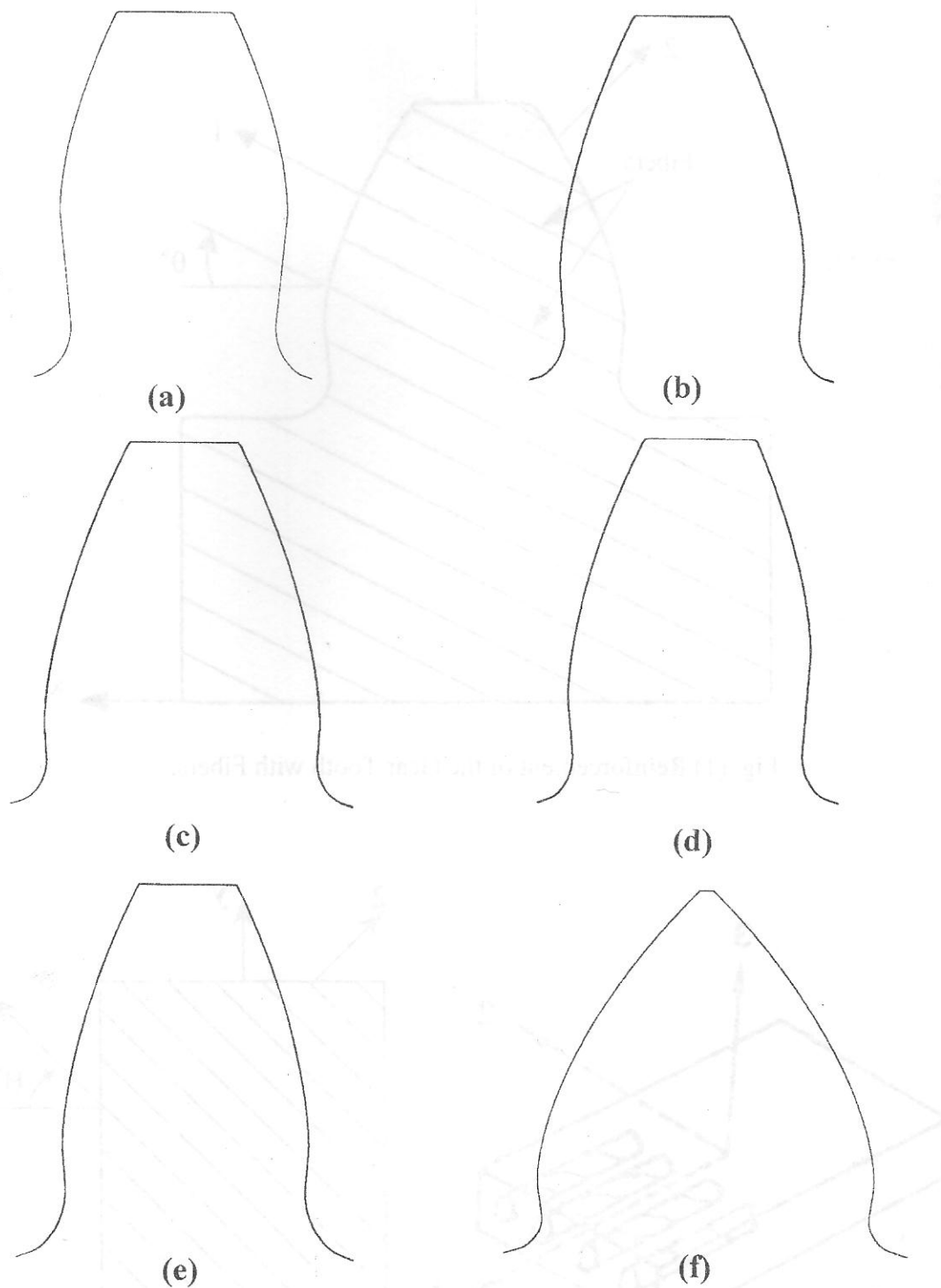


Fig. (4) Samples of Gear Tooth Profiles of module  $m_o = 10$  mm.

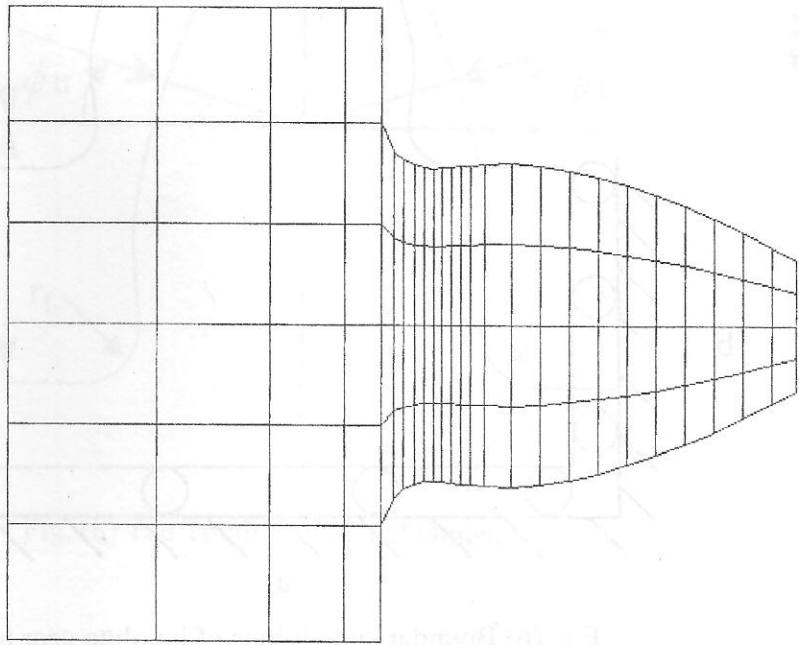
- (a)  $\phi_l = \phi_u = 14.5^\circ$ ,  $Z=14$  tooth,  $r_f = 0.3 m_o$  and  $x = 0$   
 (b)  $\phi_l = \phi_u = 20^\circ$ ,  $Z=19$  tooth,  $r_f = 0.3 m_o$  and  $x = 0$   
 (c)  $\phi_l = \phi_u = 20^\circ$ ,  $Z=24$  tooth,  $r_f = 0.3 m_o$  and  $x = 0$   
 (d)  $\phi_l = 14.5^\circ$ ,  $\phi_u = 20^\circ$ ,  $Z=19$  tooth,  $r_f = 0.3 m_o$  and  $x = 0$   
 (e)  $\phi_l = \phi_u = 20^\circ$ ,  $Z=19$  tooth,  $r_f = 0.4 m_o$  and  $x = 0$ .





(f)  $\phi f = \phi u = 14.5^\circ$ ,  $Z=14$  tooth,  $r_f = 0.3 m_0$  and  $x = 0.56$

(a)  $\phi f = \phi u = 20^\circ$ ,  $Z=19$  tooth,  $r_f = 0.3 m_0$  and  $x = 0$ .



(b)  $\phi f = 14.5^\circ$ ,  $\phi u = 25^\circ$ ,  $Z=19$  tooth,  $r_f = 0.3 m_0$  and  $x = 0$ .

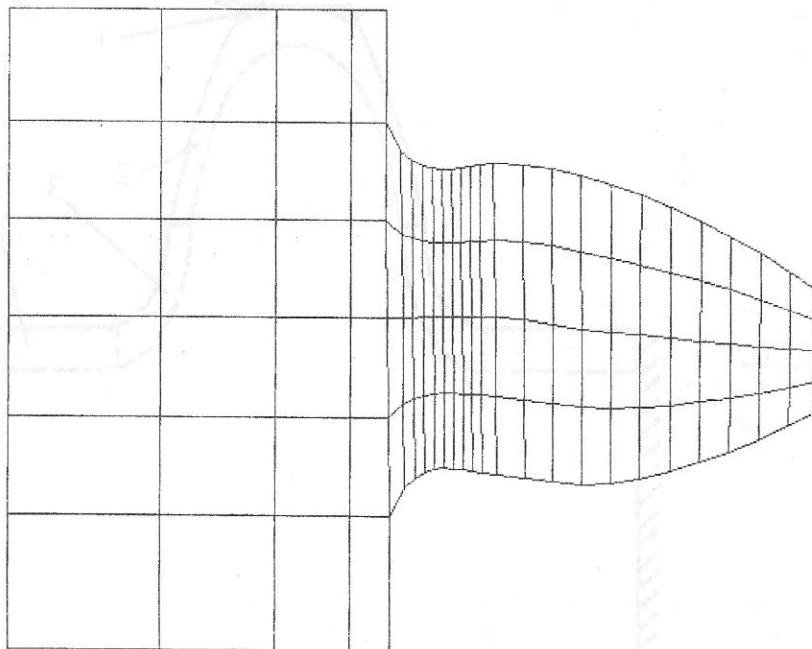


Fig. (5) Samples of Gear Tooth Mesh of Module  $m_0 = 10$  mm.

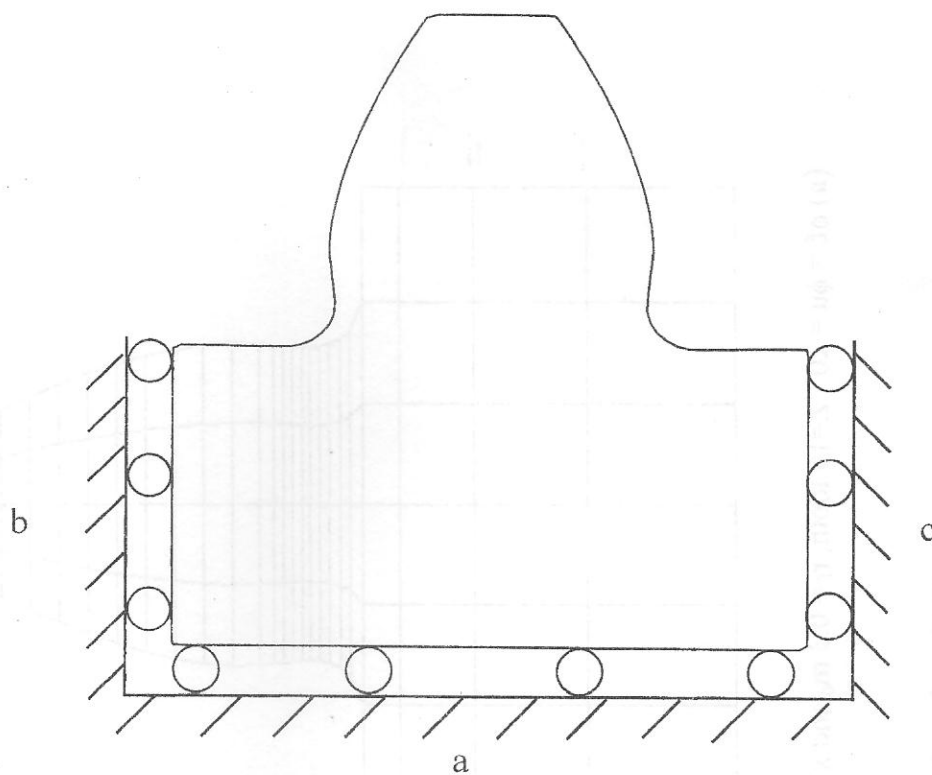


Fig. (6) Boundary conditions of involute gear tooth.

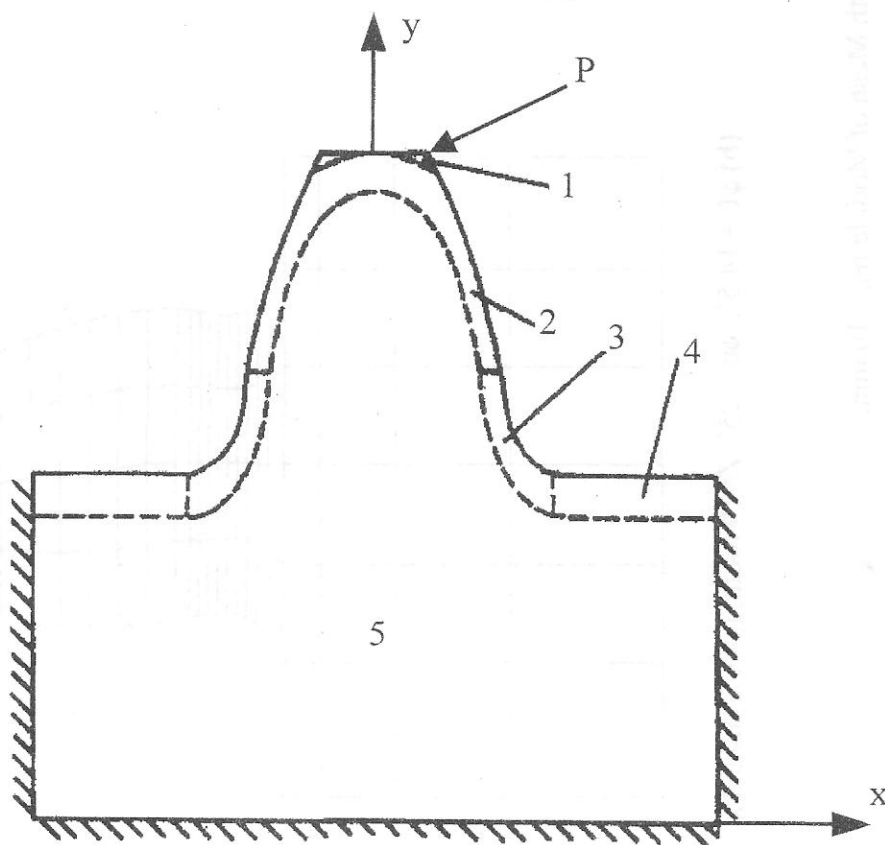


Fig. (7) Gear Tooth Model

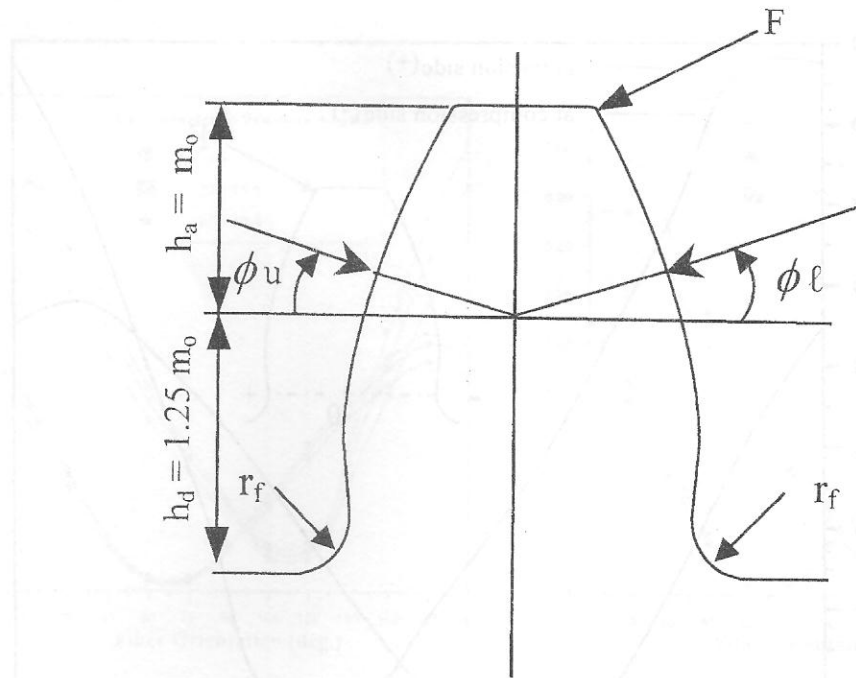


Fig. (8) The Tooth Profile and Dimensions.

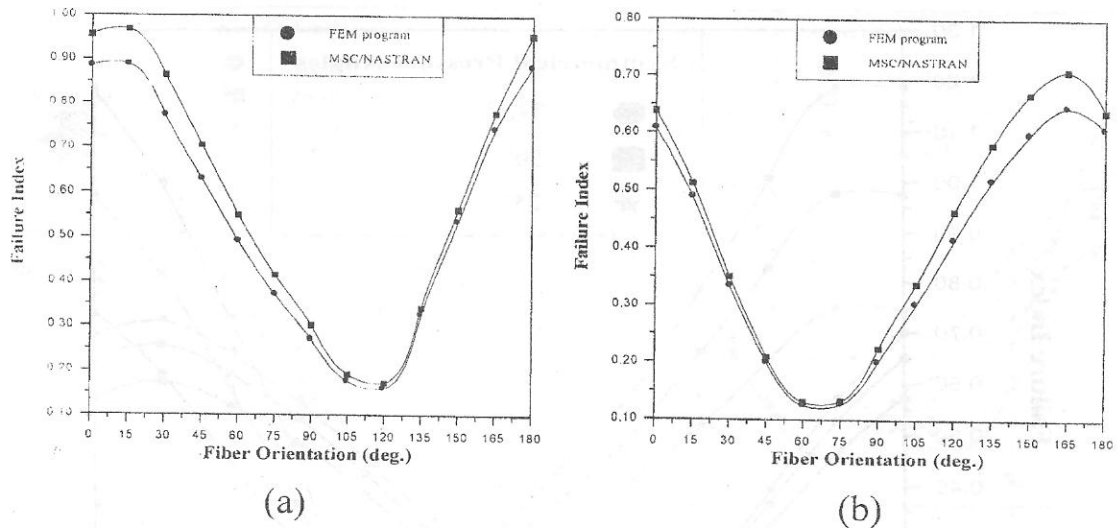


Fig. (9) Variation of Failure Index with Fiber Orientation at (a) Tension Side and (b) Compression Side.

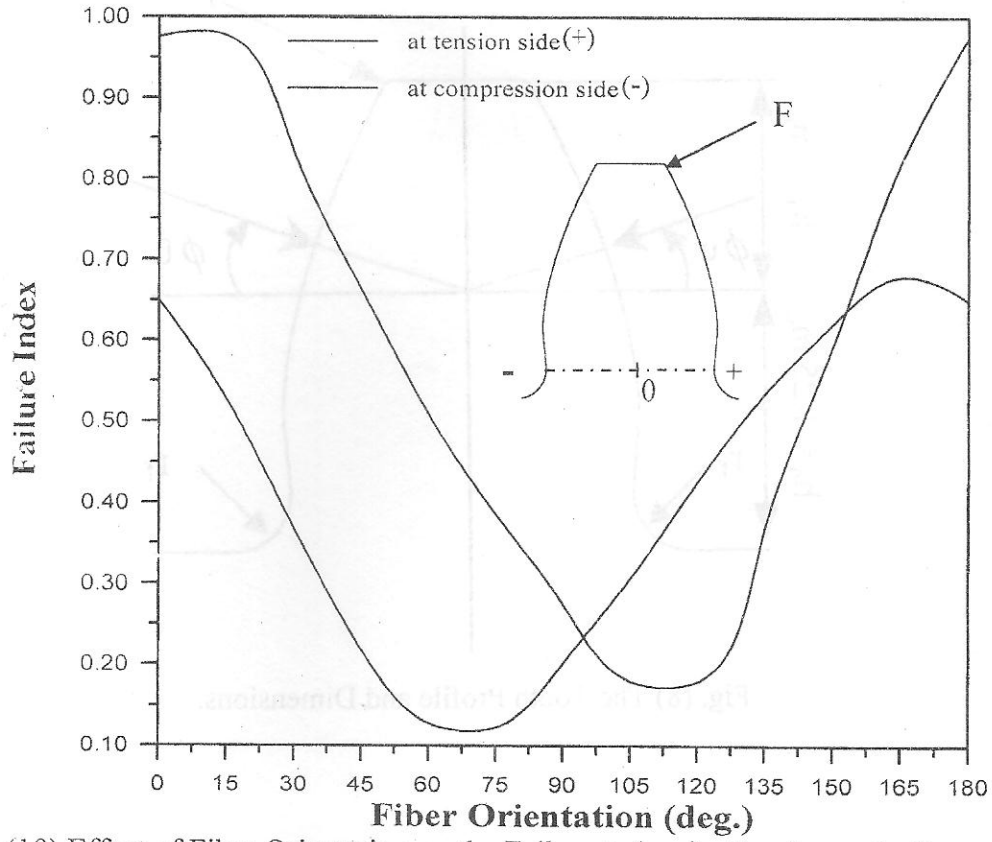


Fig. (10) Effect of Fiber Orientation on the Failure Index for Tension and Compression Sides, for  $\phi_l = \phi_u = 20^\circ$ ,  $Z=14$ ,  $r_f=0.3 m_0$  and  $x=0$ .

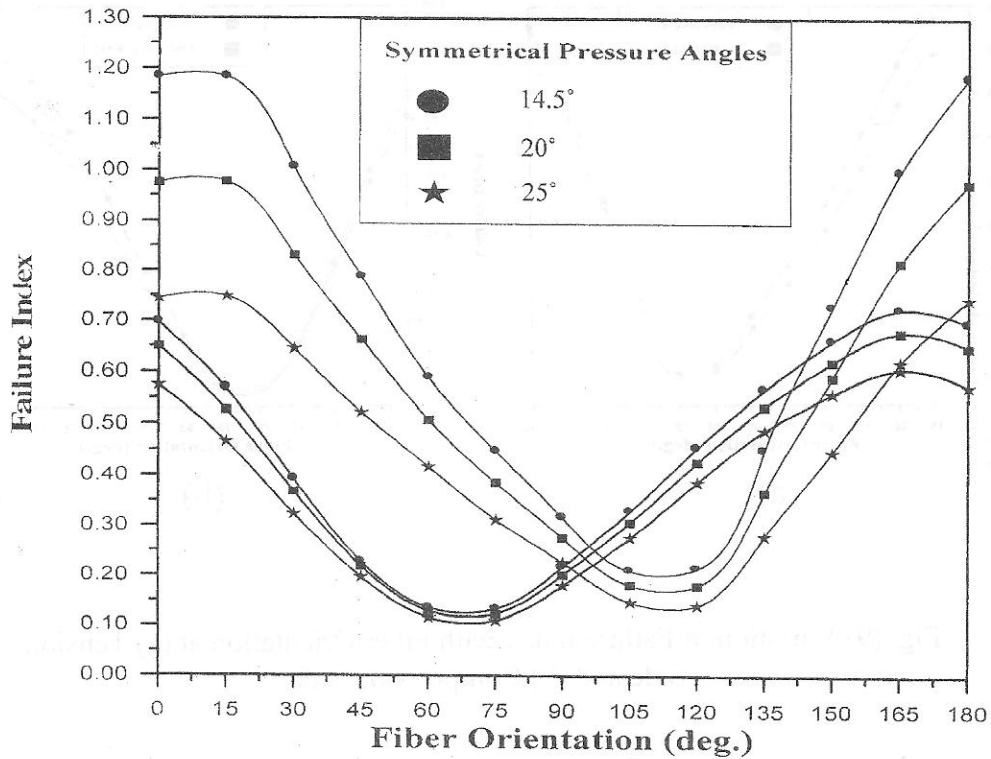


Fig. (11) Variation of Failure index with Pressure angle and Fiber Orientation, for  $Z=14$ ,  $r_f=0.3 m_0$  and  $x=0$ .



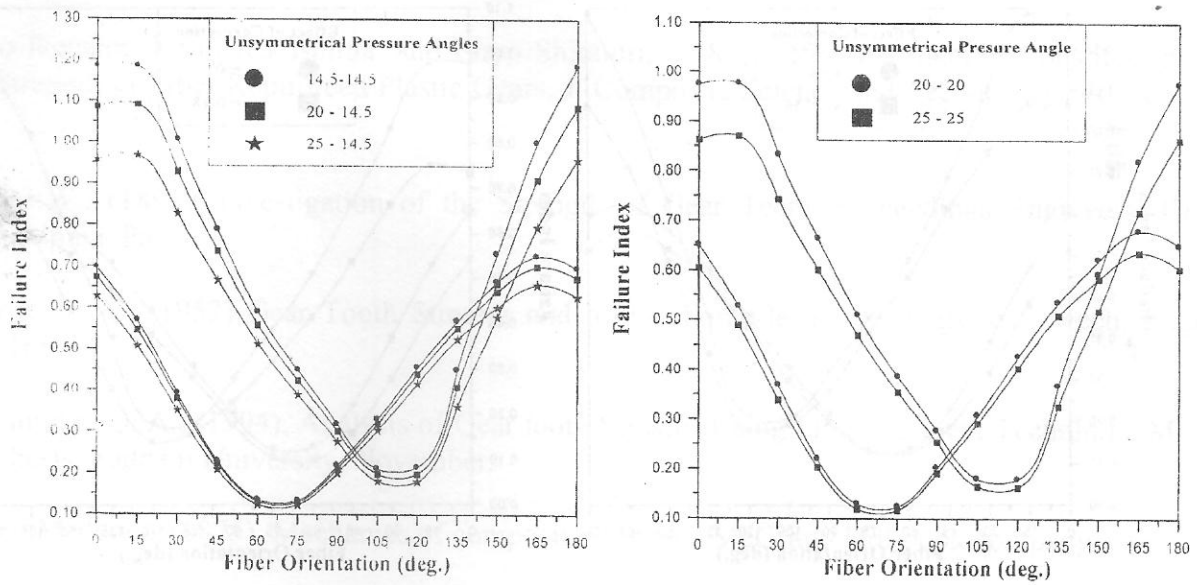
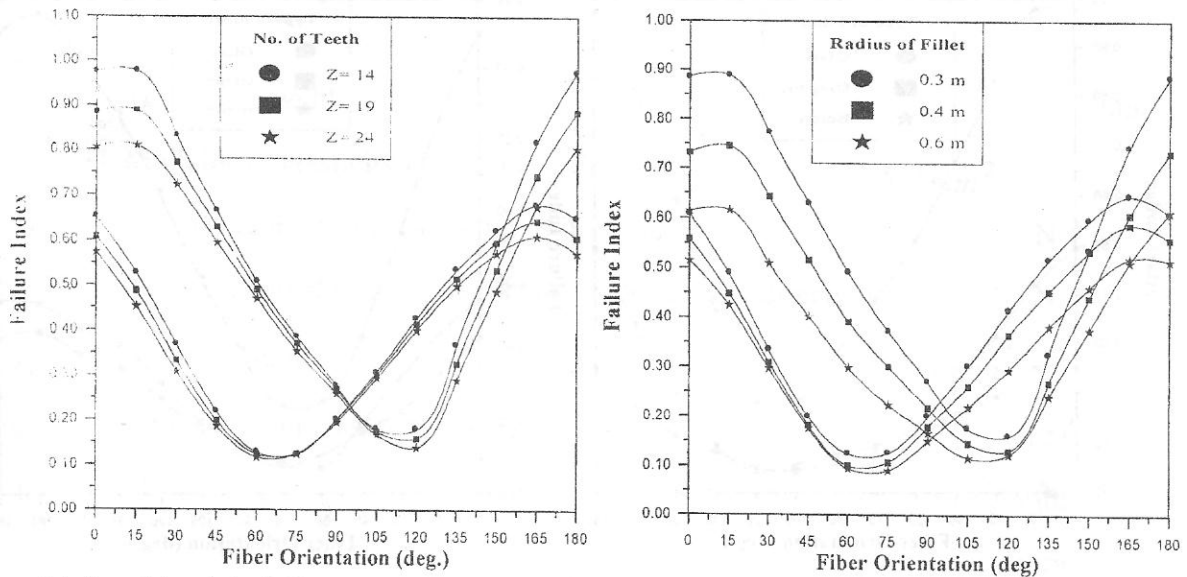


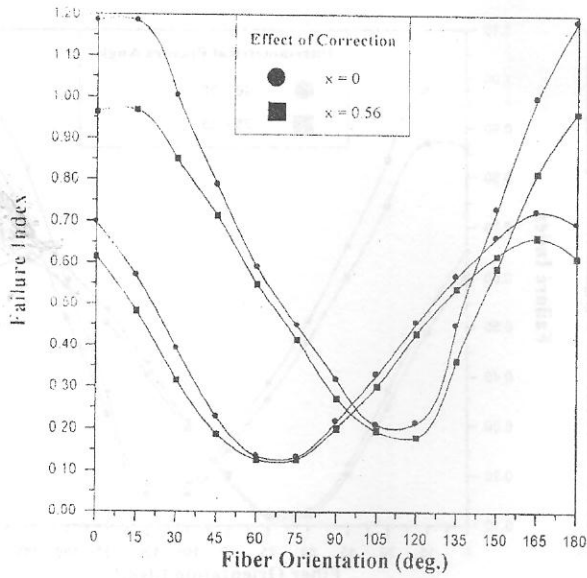
Fig. (12) Variation of Failure Index with Unload Pressure Angle and Fiber Orientation,  $Z=14$ ,  $r_f=0.3 m_0$  and  $x=0$ .



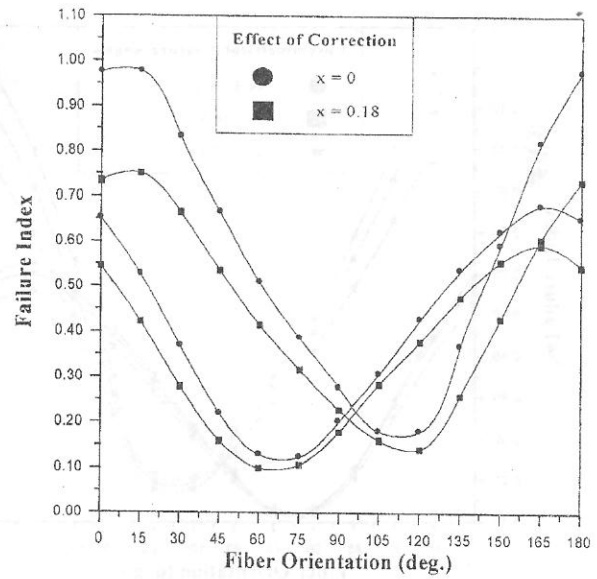
(a) for  $\phi \ell = \phi u = 20^\circ$ ,  $r_f=0.3 m_0$  and  $x=0$ .

(b) for  $\phi \ell = \phi u = 20^\circ$ ,  $Z=19$  and  $x=0$ .

Fig. (13) Variation of Failure Index with (a) Number of Teeth, (b) Radius of Fillet and with Fiber Orientation.

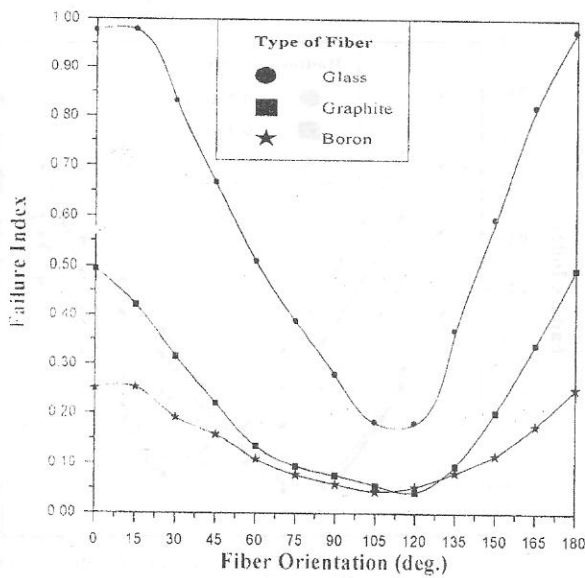


(a) for  $\phi \ell = \phi u = 14.5^\circ$ ,  $Z=14$  and  $r_f=0.3 m_o$ .

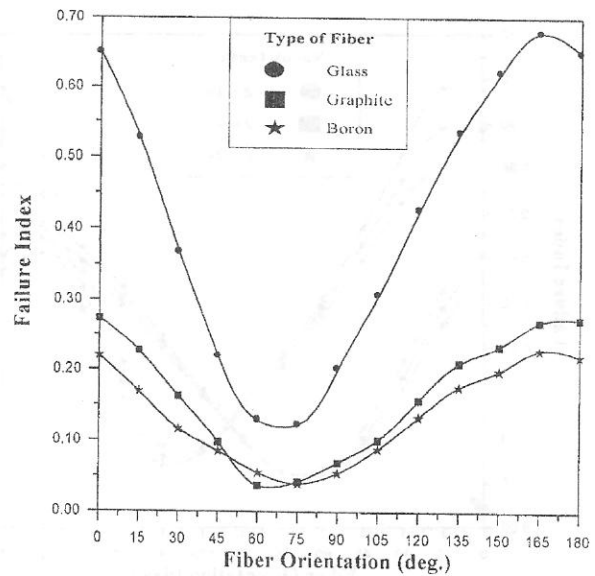


(b) for  $\phi \ell = \phi u = 20^\circ$ ,  $Z=14$  and  $r_f=0.3 m_o$ .

Fig. (14) Variation of Failure Index with Correction and Fiber Orientation.



(a)



(b)

Fig. (15) Variation of Failure Index with Type of Fiber and Fiber Orientation at (a) Tension Side, (b) Compression Side for  $\phi \ell = \phi u = 20^\circ$ ,  $Z=14$ ,  $r_f=0.3 m_o$  and  $x=0$ .



## REFERENCE

Dolan, T. J., and Broghamer, E. L., (1942), A Photoelastic Study of Stresses in Gear Tooth Fillets, University of Illinois Engineering Experiment Station, Bulletin No. 335,.

Kozo Ikegami, Kenji Kikushima, and Eiryō Shiratori, (1986), Effect of Material Constitutions on the Strength of Fiber Reinforced Plastic Gears, J. Composite Science and Technology, Vol. 27, , P. 43.

Lewis. W.. (1893), Investigation of the Strength of Gear Teeth, Proceedings Engineers' Club, Philadelphia. Pa.,.

Merritt. H. E., (1952) Gear Tooth Stresses and Rating Formula, Proceedings Inst. Mech. Engrs., Vol. 166,.

Mohammad Q. A., (1994), Analysis of Gear tooth Stresses Using Finite Element Technique, M. Sc. Thesis. Saddam University, November.

Robert M. Jones, (1975), Mechanics of composite material, McGraw- Hill book company,.

## NOTATIONS

Matrix and Vectors

[S] Strain-stress relation in principal material direction.

[Q] Reduced stiffnesses matrix.

$[\bar{Q}]$  Transformed reduced stiffnesses matrix.

Variable

b	Tooth face width.		mm
$E_1, E_2, E_3$	Modulus of elasticity in 1, 2 and 3 direction.	$N/mm^2$	
F	Normal applied force at the tip of the tooth.		N
$F_x, F_y$	Normal applied forces components in the x and y directions.		N
$G_{12}, G_{23}, G_{13}$	Shear modulus.	$N/mm^2$	
$h_a, h_d$	Addendum and dedendum heights.		mm
$m_n$	Module.		mm
$R_a$	Radius of addendum circle.		mm
$R_b$	Radius of base circle.		mm
$R_d$	Radius of dedendum circle.		mm
$r_f$	Fillet radius.		mm
S	Shear strength in the (1-2) plane.	$N/mm^2$	

X	Correction Factor.	
$X_t (X_c)$	Axial tensile (compressive) strength in the 1-direction.	$N/mm^2$
$Y_t (Y_c)$	Transverse tensile (compressive) strength in the 2-direction.	$N/mm^2$
Z	Number of gear teeth.	

Greek Letters

$\theta$	Angle of fibers inside the gear tooth domain (deg.)
$\beta$	Loading angle of the normal applied force (deg.).
$\varepsilon_1, \varepsilon_2, \varepsilon_3$	Normal strains in the principal material directions.
$\varepsilon_x, \varepsilon_y, \varepsilon_z$	Normal strains in the coordinate directions.
$\sigma_1, \sigma_2, \sigma_3$	Normal stresses in the principal material directions.
$\sigma_x, \sigma_y, \sigma_z$	Normal stresses in the coordinate directions.
$\gamma_{12}, \gamma_{23}, \gamma_{13}$	Shear strains in the principal material directions.
$\gamma_{xy}, \gamma_{yz}, \gamma_{xz}$	Shear strains in the coordinate directions.
$\nu_{12}, \nu_{23}, \nu_{13}$	Poisson's ratio in the principal material directions.
$\nu_{xy}, \nu_{yz}, \nu_{xz}$	Poisson's ratio in the coordinate directions.
$\phi_t, \phi_u$	Pressure angles for loaded and unloaded sides (deg.)